GIDL: Generalized Interference Detection and Localization System

Konstantin Gromov, Dennis Akos, Sam Pullen, Per Enge, and Bradford Parkinson
Department of Aeronautics and Astronautics, Stanford University, Stanford, CA

BIOGRAPHY

Konstantin Gromov obtained an M.S. degree in Electrical Engineering in Leningrad Electrical Engineering Institute in 1992, B.S. degree in mathematics from Leningrad State University in 1991, and M.S. degree in Astronautics and Aeronautics at Stanford University in 1994. Currently, he is working on his Ph.D. degree in Aeronautics and Astronautics at Stanford University under Prof. Bradford Parkinson. As an undergraduate and graduate student, he has worked on variety of topics involving GPS, in particular LAAS.

Dr. Dennis M. Akos completed the Ph.D. degree in Electrical Engineering at Ohio University, conducting his graduate research within the Avionics Engineering Center. After graduating he has served as a faculty member with Luleå Technical University, Sweden and is currently a research associate with the GPS Laboratory at Stanford University. His research interests include GPS/CDMA receiver architectures, RF design, and software radios.

Dr. Sam Pullen completed his Ph.D. in Aeronautics and Astronautics at Stanford University, where he is now the Technical Manager of Stanford's Local Area Augmentation System project. His research includes performance prediction, optimal system architectures, and integrity algorithms for both the Wide Area and Local Area Augmentation Systems.

Dr. Per Enge is an Associate Professor in the Department of Aeronautics and Astronautics at Stanford University. He received his Ph.D from the University of Illinois. Prof. Enge's research currently centers around the use of GPS as a navigation sensor for aviation.

Dr. Bradford W. Parkinson is the Edward C. Wells Professor of Aeronautics and Astronautics at Stanford University. He served as the first Program Director of the Joint Program Office and was instrumental in GPS system development.

ABSTRACT

The Local Area Augmentation System (LAAS) and the Wide Area Augmentation System (WAAS) are being developed by the U.S. Federal Aviation Administration (FAA) to provide satellite navigation performance compliant with the stringent requirements for aircraft precision approach and landing. A primary design goal of both systems is to insure that signal-in-space failures are detected by ground facilities and affected measurements are excluded before differential corrections are broadcast to users. One such failure is unintentional interference or intentional jamming in the GPS frequency band. To protect integrity, LAAS and WAAS ground facilities must quickly detect the presence of interference that fall within the restricted zone defined by LAAS and WAAS system requirements and thus may be hazardous to users. To protect availability, ground personnel must also be able to locate and deactivate the interference source.

To serve this purpose, Stanford University developed and tested a 1-D Interference Direction Finding system and reported its results at ION GPS-99. This prototype demonstrated the ability to locate wideband interference sources to within a few centimeters along a 12-meter track between the two IDF antennas. This system has been significantly expanded and enhanced to form the Generalized Interference Detection and Localization System (GIDL) prototype, which includes four antennas and RF sections slaved to a common clock to allow three-dimensional interference location. Measurements of differential signal propagation delays across the multiple baselines between the GIDL antennas are combined to estimate the location of the undesired signal transmitter in a manner analogous to GPS position determination. The GIDL can be implemented in parallel with a three or four-receiver LAAS ground facility (sharing

some components with the LAAS reference receivers and processors) or as a separate installation to support nearby LAAS sites and WAAS approaches.

This paper describes the GIDL receiver design and derives theoretical predictions of the ability of the GIDL to accurately locate interference sources. For the "star" configuration of GIDL antennas, where the antennas are separated by 100 meters (as would be typical of a LAAS ground facility), the GIDL should be able to locate a relatively strong interference source 3 km from the center of the GIDL antennas to within 100 meters longitudinally and 5 meters laterally. Better accuracy can be obtained from longer antenna separations. In addition, the paper includes test results from a real-time demonstration of the GIDL system in a large field on the Stanford campus. In this test, a calibrated wideband noise source at -70 dBW/MHz is moved around the field between a set of pre-calibrated locations, and the real-time GIDL display provides up-to-date estimates of the location of this noise source to within the limits predicted by the accuracy analysis. Further testing with a wider variety of interference sources is planned in the near future.

INTRODUCTION

The Local Area Augmentation System (LAAS) is a ground-based differential GPS system being implemented by the Federal Aviation Administration (FAA) for aircraft precision approach and landing. LAAS will adequately provide Category I service for those airports that are not covered by the FAA's Wide Area Augmentation System (WAAS) and is intended to provide Category II and Category III performance in the future [1]. A primary design goal for LAAS is to insure that failures occurring in the ground or space segments of GPS be eliminated by the ground system before differential corrections are broadcast to users. One such failure is unintentional interference or intentional jamming in the GPS frequency band. To protect integrity, the ground and air must quickly detect the presence of interference. To protect availability, ground personnel must also be able to locate and disable the interference source. The GIDL system would be able to assist ground personnel in finding interference sources, by providing estimated locations of any interfering signals that lie outside the tolerable LAAS interference environment, which is specified in Appendix H of the RTCA LAAS MASPS [2].

In order to serve this purpose, a specialized prototype known as GIDL has been developed. GIDL can improve LAAS availability by accurately estimating the location of the source, particularly its direction from the GIDL location. GIDL activities can be implemented in parallel with reference receiver functions and could share components with the reference receivers and processors in LAAS ground stations.

Receiver	Mnf.	Lost 1 SV, m	No pos. fix, m	All SVs Reacq., m
Survey	A	10	0	17
Survey	B	12	5	20
Survey	B	9	3	11
LAAS Ref.	A	15	3	19
LAAS Ref.	C	4	4	7
LAAS Ref.	C	12	6	18
LAAS Ref.	C	20	8	10
Military (C/A)	B	4	2	7
Consumer	C	6	4	7
Aviation	B	27	14	19
Aviation	B	12	6	14
Consumer	B	9	6	11
Automotive	B	N/A	4	N/A

Table 1: Receiver Jamming Test Results

There are several ways to implement sources of interference localization: interferometry, time-of-arrival differential system, spatial spectrum estimation, phase antenna array, etc. Multiple direction and location finding algorithms can share common hardware. Significant work has been done on estimating direction of the arrival of signals. This subject has been studied almost since invention of the radio. There are significant number of algorithms which could be used in the GIDL system.

At Stanford University, an ongoing effort is focused on research, development, implementation, and testing of LAAS architectures and architecture subsystems. This paper continues to consider the development of the GIDL receiver and algorithms as an adjunct to the Stanford LAAS prototype. Currently, most of our efforts concentrated on the interferomerical, or time-of-arrival techniques. Analysis and experimental results are described in this paper.

We have also tested a number of GPS receivers to the succeptability of interference to have a bench mark on range of the jammer. The interference source which has been used for the test is a white noise source with power of -70 dBW/MHz. Results of this experiment are present in the Table 1. The interference source was moved closer to the receiver, and the jammer location where the first satellite and all satellites are lost has been recorded. Then, the jammer was moved away from the receiver, and we recorded the range when all the satellites were reacquired. These results show that at a range of about 10 meters, this jammer becomes a threat. We can scale this results to a jammer of a different power.

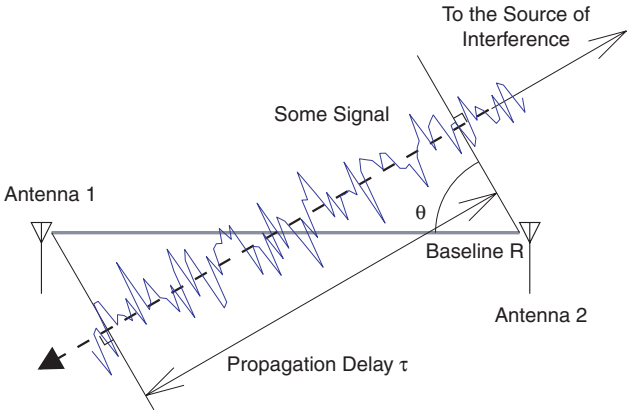

Figure 1: GIDL Concept — Interferometry

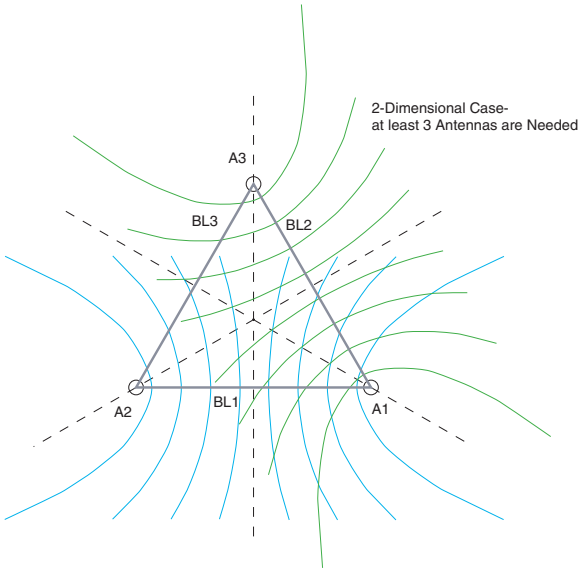

Figure 2: GIDL Idea "Inverted Loran"

GIDL THEORY

One idea for localization, known as an "interferometrical" approach, illustrates the concept and simple algorithms for direction finding. Assume that the source of interference is located far from the reception antenna so that we can assume planar wavefronts. Interfering signal propagation would hit Antenna 2 first and then with some propagation delay it would enter Antenna 1, as illustrated in Figure 1. If we can somehow estimate this propagation delay τ, from simple trigonometry we would be able estimate the direction to the signal source. There is an ambiguity associated with the single baseline, regarding which side of the baseline the source is located, but this ambiguity can be simply resolved using multiple baselines. For many signals, it is possible to estimate propagation delay τ by correlating signals received by Antenna 1 and Antenna 2.

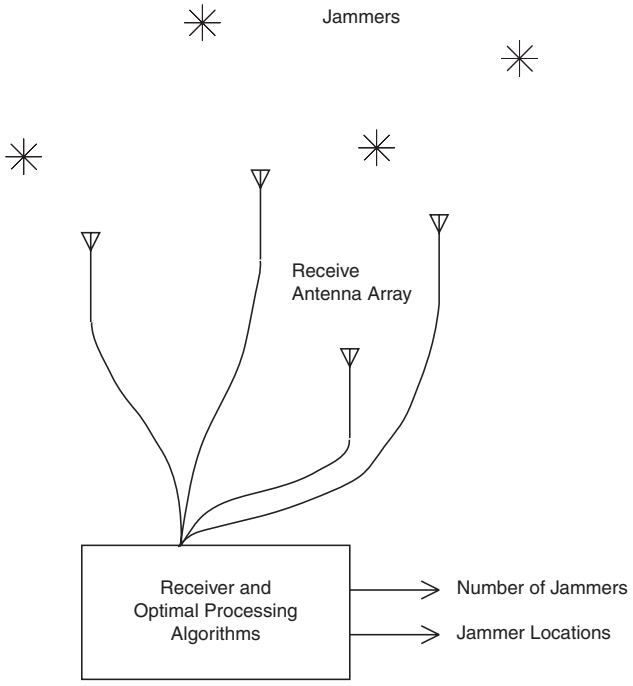

Figure 3: GIDL Realization Concept

Another idea, which we call "inverted Loran", also is quite easy to grasp, and it does not need the assumption of planar wavefronts, as shown in Figure 2. In this case, measurements include signal propagation delay times between each pair of antennas. For each baseline, the measured propagation delay would correspond to a hyperbola of possible jammer locations. Two baselines would generate two such hyperbolas. By finding their intersection, we would be able to estimate jammer location. There is an ambiguity in this technique, as in the general case two hyperbolas could intersect at two points, but it is possible to resolve this ambiguity by various techniques, for example by adding extra baselines.

GIDL HARDWARE OVERVIEW

One of the ways to build a prototype of such a system is shown in Figure 3. It is possible to build a receiver with four RF sections (i.e. with ability to connect to four antennas). It would be operated from one common clock, so it would be a completely coherent system. There are some limitations to this prototype. Namely, it would have only four antennas, and the antenna locations would be limited by cable length from the receiver to the antenna.

This section summarizes the GIDL prototype hardware that we have built and tested. For a more detailed description please see our previous paper [3]. The GIDL receiver is implemented with a single analog down-conversion/mixing

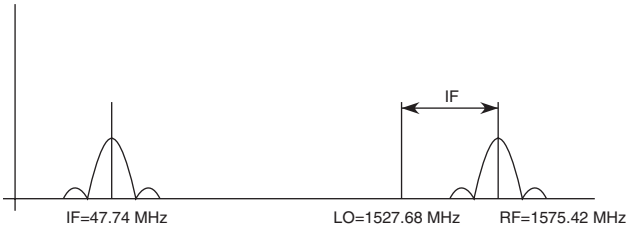

Figure 4: GIDL Frequency Plan: Analog Mixing

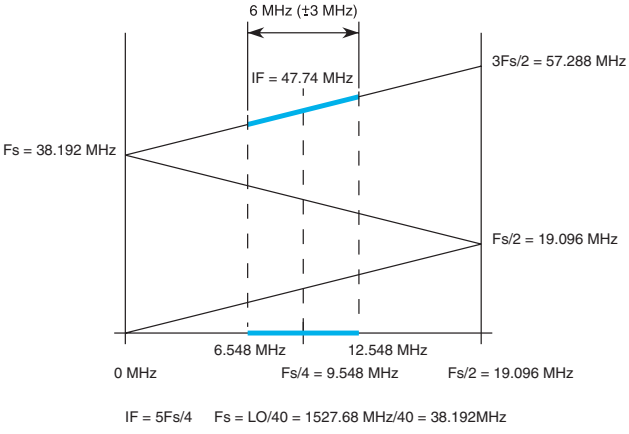

Figure 5: GIDL Frequency Plan: Sampling With Aliasing

stage. A second down-conversion is done by aliasing during A/D conversion. The remainder of the signal processing is completely digital. The system RF bandwidth is 24 MHz, and the IF bandwidth is 6 MHz, with a possible expansion to 17 MHz to protect wideband LAAS reference receivers (see Figure 4 and Figure 5).

The GIDL hardware setup is depicted in Figures 6, 7, and 8. A picture of the completed system is shown in Figure 9. An aluminum chassis hosts the RF/IF downconversion stages, master clock and synthesizer, and power supply. The A/Ds are PCI cards which are installed into a data processing PC, which is set up below the RF/IF stages. In the picture in Figure 9, only antenna 1 and antenna 2 inputs are connected.

EXPECTED SYSTEM PERFORMANCE

There are two major characteristics to the GIDL system: (1) maximum range and coverage; (2) the accuracy of the jammer location. The first describes what maximum range the system should be able to detect a jammer of a given power, and that range better be greater than effective radius of the jammer. Another characteristics describes how accurately we can locate the jammer if we can detect it. In this section we look at both characteristics, state expected performance, and list aspects which can improve it.

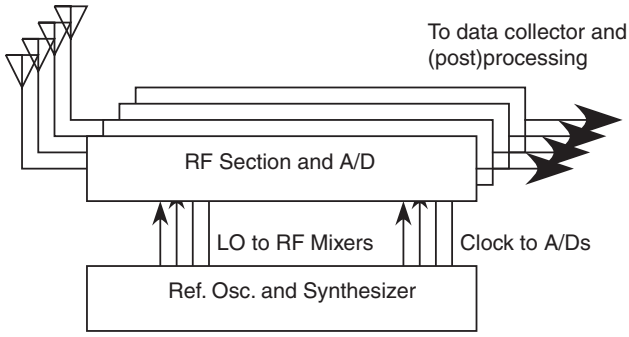

Figure 6: Diagram of GIDL Hardware Setup

Figure 7: Diagram of RF Section and A/D

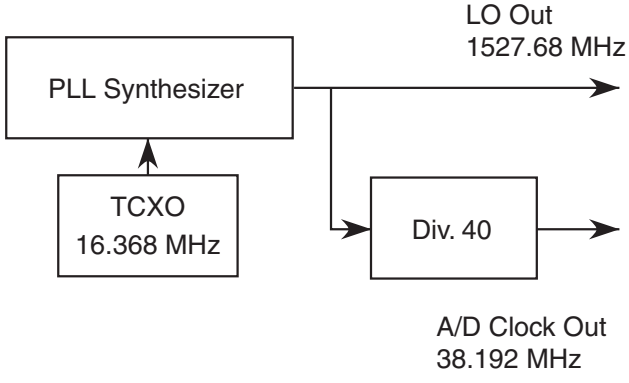

Figure 8: Common Clock Diagram

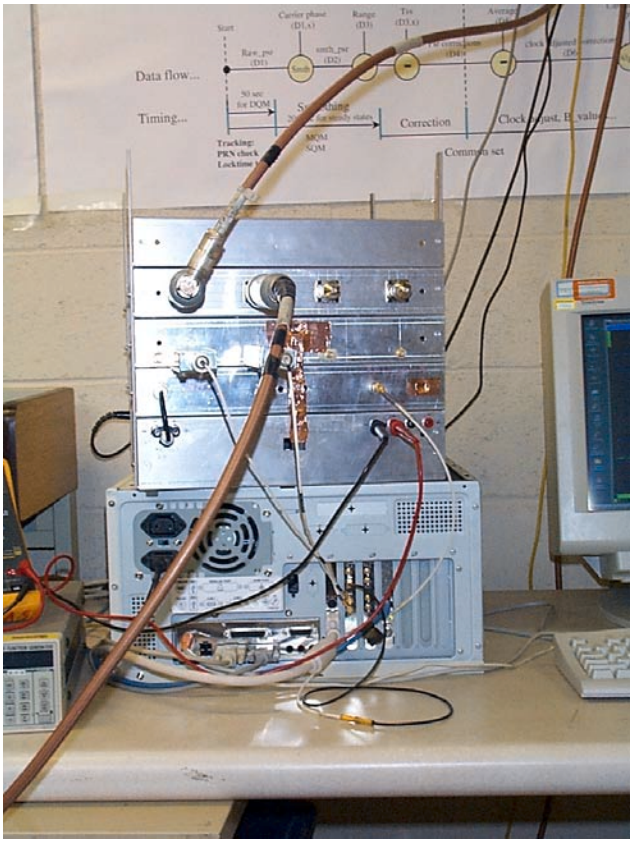

Figure 9: Picture of the Completed GIDL Receiver

Maximum range and coverage of the system is determined by looking at the post-processing signal-to-noise ratio of the received signals. That ratio is defined by setting probabilities of detection and false alarm.

Assume that we have a single baseline system as shown in Figure 10. Assuming that the desired post-processing SNR ($q^2_{\text{out cor}\,ik}$) is set than using link equation we can derive that for an antenna pair A_i, A_k, the maximum range and coverage determined by

$$\|\mathbf{R}-\mathbf{L}_i\|^2\|\mathbf{R}-\mathbf{L}_k\|^2 \le F^4_{1\,ik},$$

or

$$\frac{q_{\text{out}\,i}q_{\text{out}\,k}}{q^2_{\text{out cor}\,ik}} \ge 1.$$

Where

$$F^4_{1\,ik} = \gamma_i\frac{(NG)G_i\lambda^2}{4\pi kT_{\text{eff}\,i}}\cdot\gamma_k\frac{(NG)G_k\lambda^2}{4\pi kT_{\text{eff}\,k}}\cdot\frac{1}{q^2_{\text{out cor}\,ik}} = \frac{(NG)^2G_iG_k\lambda^4\gamma_i\gamma_k}{(4\pi)^2k^2T_{\text{eff}\,i}T_{\text{eff}\,k}q^2_{\text{out cor}\,ik}}.$$

This equation describes Cassini's ovals with the center at the center of the baseline between two antennas. For long ranges these ovals approximate circles.

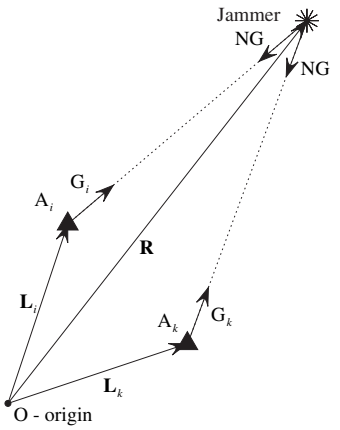

Figure 10: Single Baseline System

Equation 1 is the general equation, let's see what results we would get if we plug in some numbers which are of interest to us. In Figure 12 the maximum range and coverage for specific baselines and jammer powers are plotted. Figure 11 shows antenna array configuration which has been used to generate each plot. This is the so called "Star Antenna" configuration where master antenna is located in the center and three other antennas are located on some distance from the central antenna and spaced 120^o apart. This configuration produces three independent baselines, on the each plot three Cassini's ovals are shown, one per each baseline, intersection of these ovals is the coverage of the whole system. The top row of the plots corresponds to the baselines of 12 meters long, with the bottom row to the baselines of 100 m. Note that for the weakest jammer and 100 m baseline there is no coverage. The jammer is simple too weak to be detected by two antennas simultaneously with the given system parameters. Other assumptions which used in generation of this plots: $G_i = G_k = 1$ — Antennas are omnidirectional with unity gain; postprocessing SNR $q^2_{\text{out corr}} = 50$ and it is set by probability of detection $P_d \approx 0.75$ and probability of false alarm $P_{fa} = 10^{-6}$); background white noise is $kT_{\text{eff}} = 4\cdot 10^{-21}$ W/Hz; and processing losses are $\gamma_i = \gamma_k = 0.3$

Comparison of these plots with Table 1 shows that the coverage of the GIDL is larger than effective radius of the jammer, which is taken as a loss of the one satellite, and on average is about 10 m for -70 dBW/MHz jammer (it is possible to scale that number to a jammer of any power).

Everything what has been said in the previous paragraph is true for a GPS receiver using the same antennas as the GIDL system, but by using different antennas it is possible to get a differential advantage of GIDL versus a GPS receiver.

By using different antennas for GIDL and the GPS receiver

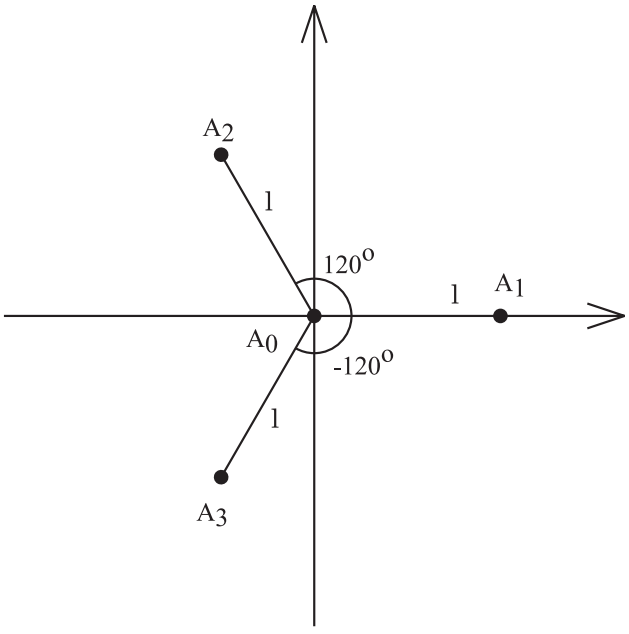

Figure 11: Antenna Configuration for Analysis

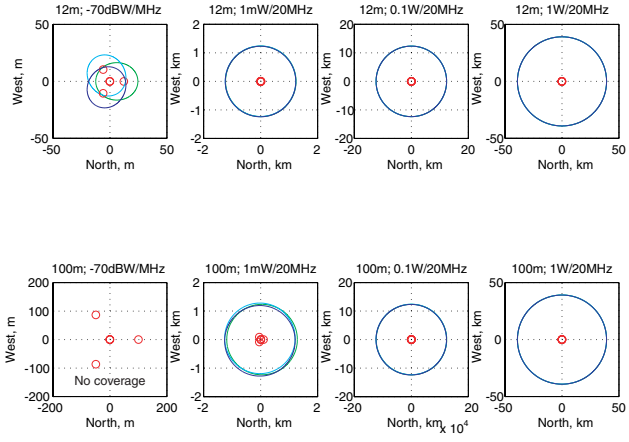

Figure 12: Maximum Range and Coverage of the GIDL System With Baselines 12 m and 100 m and Star Configuration for Jammers of Various Power

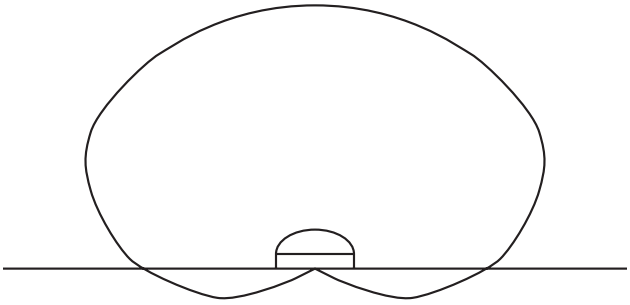

Figure 13: GPS Receiver Antenna

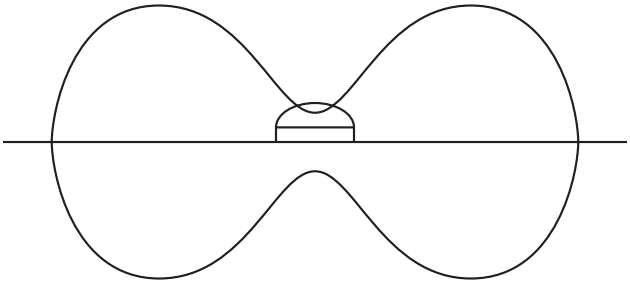

Figure 14: GIDL Antenna

it is possible to improve the range of the GIDL and lessen the effective range of the ground jammer. A typical antenna gain pattern of the GPS receiver is shown in Figure 13. It has low gain at low elevations, exactly where the jammers most likely would happen be. On the contrary if we use antenna patterns similar to that shown in Figure 14 we would get extra antenna gain in the most probable jammer direction. Thus the small gain of the GPS antenna at low elevations shrinks the jammer effective radius for GPS receiver, and the high gain of GIDL antenna in horizontal plane improves the jammer detection capability.

The Stanford experimental GIDL system has only 4 antennas, which form 3 independent baselines. Jammer locations would lie on the intersection of three hyperbolas defined by these three baselines. In this special case it is possible to derive an analytical solution for the jammer location. Four antennas would form three baselines, so three range difference ΔR_i measurements would provide:

$$\Delta R_i = R\,(1 - \sqrt{1 - \frac{2l_i}{R}(\cos\epsilon\cos\epsilon_i\cos(\beta-\beta_i) + \sin\epsilon\sin\epsilon_i) + \frac{l_i^2}{R^2}}\,),$$

with unknowns: R range to the jammer, β elevation of the jammer, ϵ elevation of the jammer; and system parameters (constants): l_i Radius-vector of the i-th antenna, β elevation of the i-th antenna, ϵ elevation of the i-th antenna.

We developed an analytical solution to the jammer position (R, β, ϵ) based on the measured signal delays ΔR_i, and known system parameters.

It is possible to estimate the error covariance matrix of possible jammer location. Jammer location ECM is defined by $B_{\rm loc} = (H^t B^{-1}_{\Delta R_i} H)^{-1}$, where $B_{\Delta R_i}$ is ECM of measurements ΔR_i, and depends on SNR in each antenna.

$$H = \frac{\partial \Delta R_i}{\partial R,\, \partial \beta,\, \partial \epsilon}$$

For a constant power jammer, depending on the jammer power and location, one would have to calculate SNR for each antenna, then compare it with the detection threshold, and only if it is above such a threshold, use it to estimate measurement errors.

In order to estimate ECM of the measurements we first would use the link equation to estimate the SNR of the jammer as seen by each antenna

$$q_i^2 = \frac{P_j G_i \lambda^2 \gamma_i}{(2\pi)^2 k T_{\text{eff}\ i} |\mathbf{R} - \mathbf{L}_i|^2}$$

And then use these estimates to calculate ECM of the measurements:

$$B_{\Delta R_i} = \frac{c^2}{\Delta f T} \frac{3}{2\pi^2 \Delta f^2} \frac{1 + q_1^2 + \ldots + q_4^2}{q_1^2 + \ldots + q_4^2} \times \left(\begin{pmatrix} \frac{1}{q_2^2} & 0 & 0 \\ 0 & \frac{1}{q_3^2} & 0 \\ 0 & 0 & \frac{1}{q_4^2} \end{pmatrix} + \frac{1}{q_1^2} \begin{pmatrix} 1 & 1 & 1 \\ 1 & 1 & 1 \\ 1 & 1 & 1 \end{pmatrix} \right)$$

Now when we know $B_{\Delta R_i}$ we can calculate ECM of the jammer location estimate: $B_{\rm loc} = (H^t B^{-1}_{\Delta R_i} H)^{-1}$, sigmas are on the diagonal.

Knowing ECM of the jammer position estimations we can plot the expected system accuracy, in terms of error ellipses. Here we present the results of the analysis for three types of the jammer (relatively strong, weak and very weak). Results are shown in the Figures 15, 16, 17. It is assumed star antenna configuration with baselines of 100m. Jammers of the specific power have been placed in the various locations around the antenna array, and a horizontal projection of the error ellipses has been plotted. Each line on the plot is actually an error ellipse, narrow in azimuthal direction and wide in the range. Thus for the relatively strong jammer one can see individual ellipses, and the resolution in range is good. For the weak jammer, we are still obtaining good azimuthal resolution, but the ellipses elongates in range direction (they start to overlap), and for the very weak jammer we plotted "x" at the range which the specified power of the jammer is undetectable.

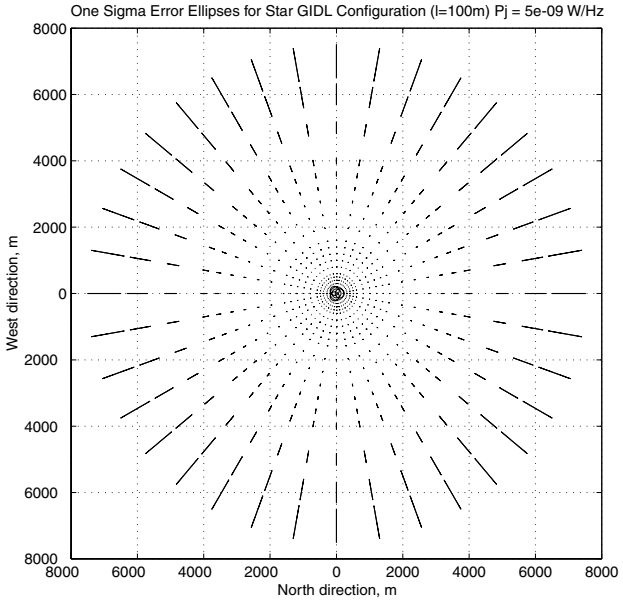

Figure 15: Error Ellipses for Constant Power Jammer: 10mW/20MHz

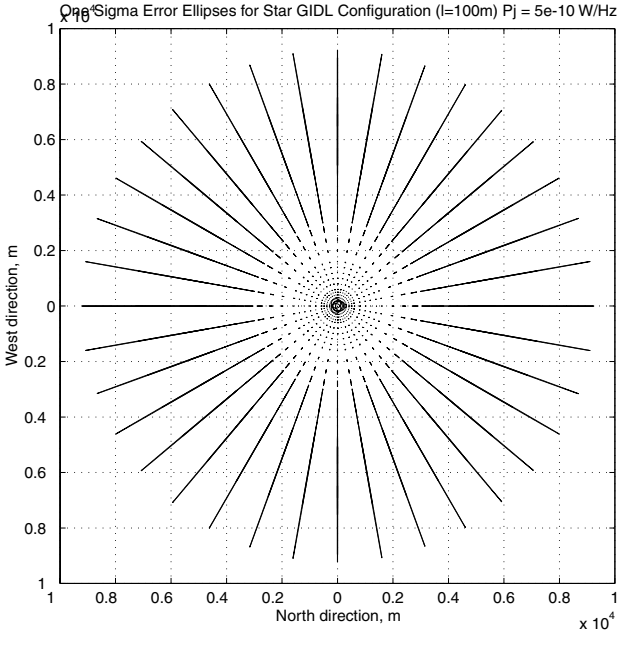

Figure 16: Error Ellipses for Constant Power Jammer: 1mW/20MHz

GIDL CALIBRATION USING GPS SIGNALS

Currently the basic GIDL measurement is TDOA of the signals to the antennas. Jammer direction and location is

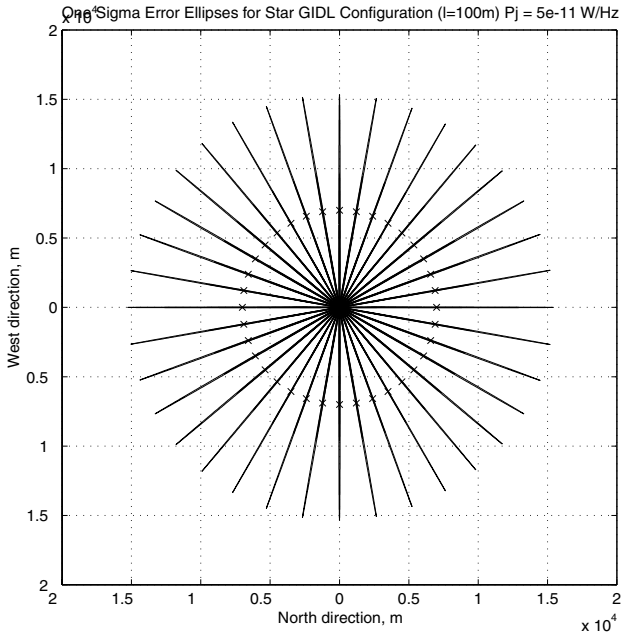

Figure 17: Error Ellipses for Constant Power Jammer: 0.1mW/20MHz

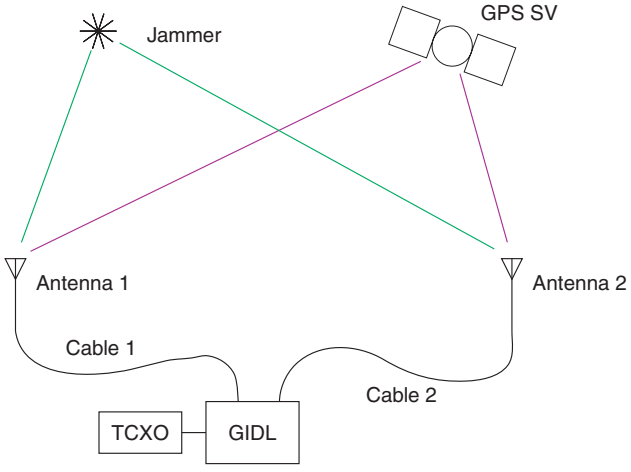

Figure 18: GIDL Calibration Setup

calculated on the basis of these measurements. These measurements have to be done relative to the antennas, so unknown delays in the cable and in the system should be calibrated out. Also because a system clock is been used to calculate propagation delay, it also has to be calibrated. Thus the major system unknowns, which should be calibrated are: relative delay in the antenna cables; offset in the master clock (TCXO); variations with temperature and other factors.

The situation exists that the jamming signal is not present a majority of the time, and GPS signal is coming from the known sources at known locations — GPS satellites. Thus we can utilize that signal to calibrate the system clock and system delays. Algorithms have been developed to utilize that signal for the calibration of the GIDL system.

EXPERIMENTS AND RESULTS

Numerous experiments have been performed with the GIDL hardware and software. Most of the effort has been on developing calibration software and performing calibration of the system. Experimental results of the system delay calibration and the clock calibration are shown in the Figure 19. Fifty data sets have been collected a few minutes apart. Each data set used to calculate system clock error and system delay. Antenna locations and satellite geometry are known, expected delay and the expected signal frequency is know. The satellite frequency is measured using our system and signal time difference of arrival calculated. Then the expected results are subtracted from the measured and the errors are plotted. The first plot shows average clock error for each given data run. Averaging is done on all satellites in view. The next plot shows average system delay and also the average of all satellites in view. The next plot shows number of satellites used, and then delay error on the basis of each individual satellite, and clock error based on each satellite measurement.

Figure 20 shows the running average of the clock estimation and running average of the delay estimation. It also shows three different ways which we are trying to estimate the top of the GPS correlation peak: maximum, discriminator function, and median. All three of these measurements are valid measurements, but we decided to go with the maximum measurement, which is least susceptible to multipath errors. Figure 21 shows a running average for the number of runs of the system delay, based on the maximum of the correlation peak measurement, and it is converging to approximately 5.75m. That error was primary defined by the cables of the different length used in that experimental setup.

This results shows that we can calibrate the system clock

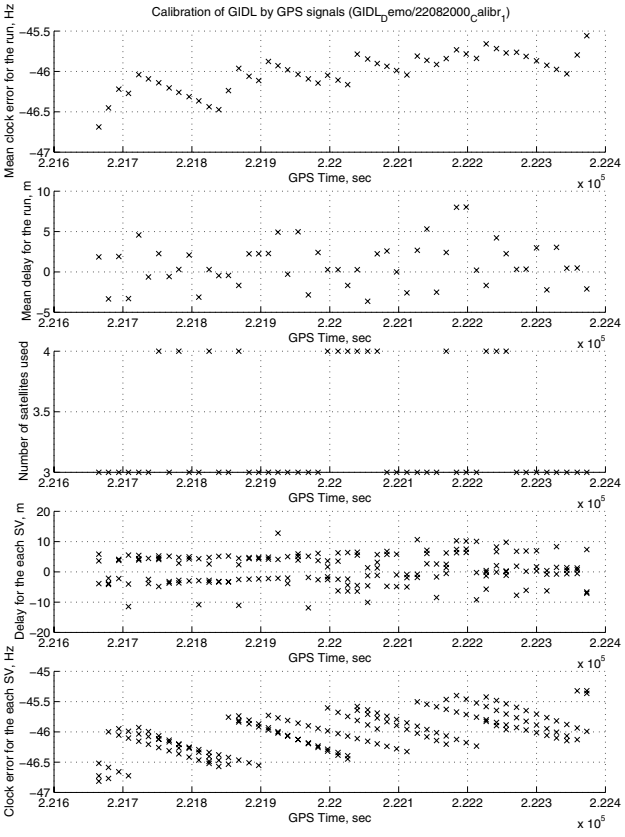

Figure 19: GIDL Calibration: Results of Clock and Delay Calibration

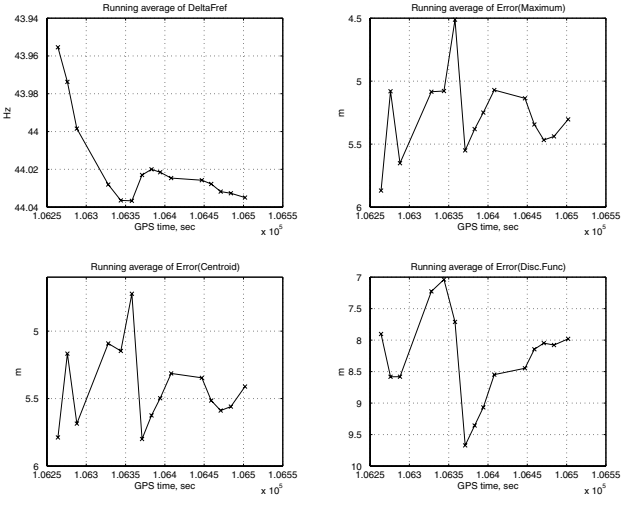

Figure 20: GIDL Calibration: Results for Data Runs 1—15; Number of SVs per Each Run: 5 5 4 4 4 6 6 5 5 4 5 5 4 4 4

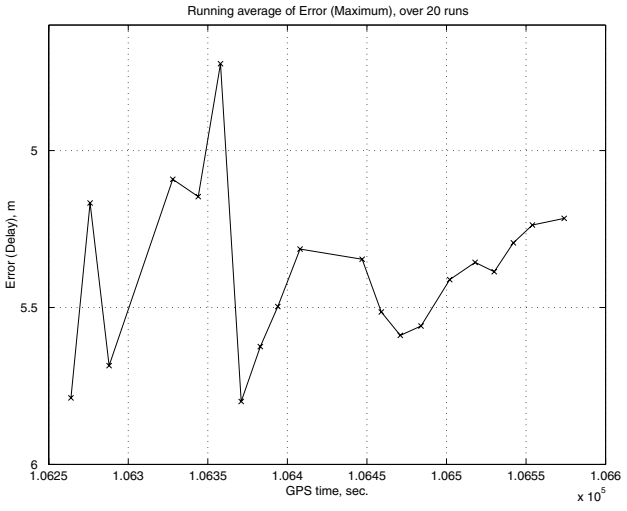

Figure 21: GIDL Calibration: Results for the 20 Data Runs

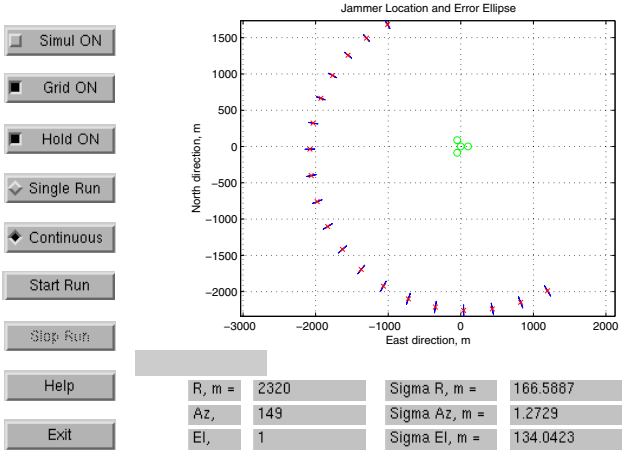

Figure 22: Real-Time GIDL Display Software (Simulation)

and system delays by the means of the GPS signals.

Another piece of software which has been developed in the lab is GIDL jammer positioning display software. It displays jammer position in the real time, and it has an option of tracking the location of the moving jammer. There is also an option to run it from simulated data or from real data. In Figure 22 the display shows locations of the jammer as they are appear in time, so it is easy to see that jammer performs spiral motion (data has been supplied by simulation code for this demonstration). In addition to jammer locations this display also indicates calculated error ellipses (which looks like a little strikes), which would assist in searching for the jammer.

Figure 23 shows results of one of the real experiments. Antennas have been set up at the bed of the dry lake Lagunita

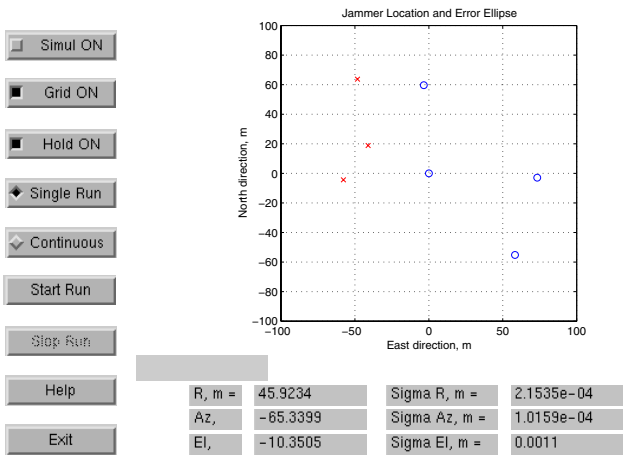

Figure 23: Real-Time GIDL Display Software (Experimental Results)

on the Stanford Campus, and their locations have been surveyed. They are marked by circles on the display. Also the locations for the jammer have been surveyed, they are marked by the "x". The system has been set up, and calibrated. Then jammers are placed in each survey location, and display shows estimated jammer location and errors. Errors and jammer location are shown in this figure. They are close to the theoretically predicted results. For the complete and certain results, as well as meaningful statistics, additional data collections are needed.

FUTURE DEVELOPMENT: CONCEPT OF DISTRIBUTED GIDL

In this paper we also would like to introduce concept of the distributed GIDL system, shown in Figure 24. This is possible extension of GIDL. In the current setup all hardware and software processing in the GIDL is colocated. So antenna configuration and coverage pattern are limited by the length of RF cables, which cannot exceed few hundred meters.

In the proposed concept of the Distributed GIDL system we would put data transmission and time synchronization on a network, which would have number of nodes — Single channel GIDL receivers, or Bit grabbers, which would collect data simultaneously, and then send it to the main processing station, or even would do preliminary processing on each node.

This system has number of the advantages compare to the original multichannel GIDL system: Each receiver is inexpensive; covers large area; can cover specific areas; easy to extend; improved accuracy due to the better geometry. But there is a major problem: how to synchronize all

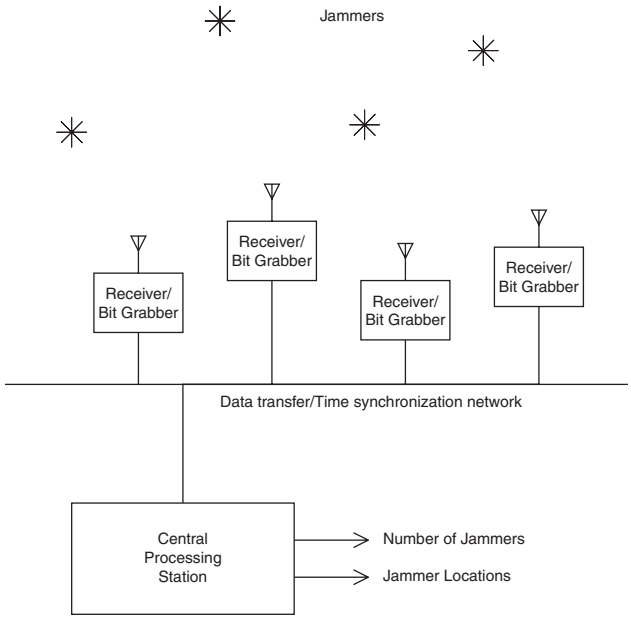

Figure 24: Distributed GIDL System

these receivers, and how to transmit large amounts of data which they are generate. Another issue is generating computationally efficient algorithms to process all this waste amount of data.

CONCLUSIONS

We have developed a 4-channel, common-clock digital receiver which operates in the L1 GPS band. The primary intended use for this receiver is Generalized Interference Detection and Localization System and development of new localization algorithms. Also jammer localization and GIDL interface display software has been developed. Experimental results correspond with predicted theoretical performance. GIDL can improve overall LAAS availability by finding direction or location of any interference sources.

FUTURE PLANS

There are a number of aspects which are planned to do with developed hardware and to improve system performance. These include: Develop short baseline direction finder and antenna array; Develop and test distributed GIDL system; Verify system performance on different types of interference sources, and different configurations of antenna arrays; Develop detection algorithms to estimate number of interferers; Develop operational procedures for GIDL operation; Integrate GIDL subsystem with Integrity Monitoring Testbed and evaluate overall system performance.

ACKNOWLEDGMENTS

We would like to thank our colleagues for the help they provide to us while we are working on the project. We also would like to thank Stanford University and academic community for the nice environment to work and communicate with people. And our special thanks to the Federal Aviation Administration for the support and funding of this project.

REFERENCES

1. Swider, R., Recommended LAAS Architecture, Presented to RTCA SC-159, WG-4, Anaheim, CA, November 12, 1996.

2. Minimum Aviation System Performance Standards for the Local Area Augmentation System. Washington, D.C.: RTCA DO-245, September 28, 1998.

3. Gromov K., et al. "Interference Direction Finding for Aviation Applications of GPS," *Proceedings of ION GPS-99,* Nashville, TN, Sept. 14-17, 1999.

4. "Coherence and Time Delay Estimation", edited by C. Carter, IEEE Press, 1993